UNIVERSIDADE DE SÃO PAULO

Instituto de Ciências Matemáticas e de Computação

Scene Segmentation of the Chaotic Oscillator Network

Liang Zhao
Elbert E.N. Macau
Nizam Omar

Nº 57

NOTAS

São Carlos - SP

UNIVERSIDADE DE SÃO PAULO
Instituto de Ciências Matemáticas e de Computação

ISSN 0103-2577

Scene Segmentation of the Chaotic Oscillator Network

Liang Zhao
Elbert E.N. Macau
Nizam Omar

Nº 57

NOTAS

Série Computação

São Carlos – SP
Jan./2001

Scene Segmentation of The Chaotic Oscillator Network

Liang Zhao[1], Elbert E. N. Macau[2], and Nizam Omar[3]

[1] Departamento de Ciência de Computação
Instituto de Ciências Matemáticas e de Computação
Universidade de São Paulo – Campus de São Carlos
Caixa Postal: 668
13560-970, São Carlos – SP, Brasil
zhao@icmc.sc.usp.br
[2] Laboratório de Integração e Testes, Instituto Nacional de Pesquisas Espaciais, Brasil
elbert@lit.inpe.br
[3] Instituto Tecnológico de Aeronáutica, Brasil
omar@comp.ita.cta.br

Resumo. Neste artigo, apresentamos uma rede de correlação oscilatória caótica para segmentação de cenários. A rede é bidimensional com elementos caóticos localmente acoplados. O modelo oferece um mecanismo para escapar do dilema de sincronização-assincronização e consequentemente, tem capacidade de segmentação não limitada. A dinâmica caótica e a sincronização caótica no modelo serão analisadas. A propriedade de assincronização é garantida pela definição do caos. As simulações do computador confirmam a predição teórica.

Abstract. A chaotic oscillatory correlation network for scene segmentation is presented. It is a two-dimensional array with locally coupled chaotic elements. It offers a mechanism to escape from the synchrony-desynchrony dilemma. As a result, this model has unbounded capacity of segmentation. Chaotic dynamics and chaotic synchronization in the model are analyzed. Desynchronization property is guaranteed by the definition of chaos. Computer simulations confirm the theoretical prediction

1 Introduction

Sensory segmentation is the ability to attend to some objects in a scene by separating them from each other and from their surroundings [23]. It is a problem of theoretical and practical importance. For example, it is used in situations where a person can separate a single, distinct face from a crowd or keep track of a single conversation from the overall noise at a party. Pattern recognition and scene analysis can be substantially simplified if a good segmentation is available.

Neuronal oscillation and synchronization observed in the cat visual cortex have been suggested as a mechanism to solve feature binding and scene segmentation problems [5, 6, 9]. Scene segmentation solution under this suggestion can be described by the following rule: the neurons which process different features of the same object oscillate with a fixed phase (synchronization), while neurons which code different objects oscillate with different phases or at random (desynchronization). This is the so-called Oscillatory Correlation [22]. The main difficulty encountered in these kinds of models is to deal with two totally contrary things at the same time: synchrony and desynchrony. The stronger the synchronization tendency among neurons, the more difficult it is to achieve desynchronization and vice-verse. Then, segmentation solutions are tradeoffs between these two tendencies. We call this situation the Synchrony-Desynchony Dilemma.

The segmentation capacity (number of objects that can be separated in a given scene) is directly related to this dilemma, i.e., the capacity will always be limited if the synchrony-desynchrony dilemma cannot be escaped from. This is because the enhancement of synchronization or desynchronization tendency will inevitably weaken another tendency. Usually desynchronization is weakened because a coherent object should not be broken up. Segmentation capacity is decided exactly by the model's desynchronization ability since the desynchronization mechanism serves to distinguish one group of synchronized neurons (an object) from another. Thus, the segmentation capacity decreases as the desynchronization tendency is weakened. It is worth noting that a model's segmentation capacity is crucial in parallel processing, such as oscillatory correlation or neural networks, since segmented patterns may appear at the same instance. So, various objects would be indiscriminately grouped if the model's capacity were highly limited.

Many oscillatory correlation models for scene segmentation have been developed [2, 10, 11, 14, 15, 16, 21, 22, 23, 24, 25]. Some works show the great potential of applications of solving real image segmentation and some perception problems [3, 26, 28]. Other works show that these kinds of models not only can be applied to the segmentation of a visual scene, but also to signal discrimination of other modalities, such as auditory segregation [24, 27]. From the viewpoint of network connection structure, these models can be classified into three categories: long-range coupling models, local coupling models and mixed coupling models.

Most of the early oscillatory correlation models are long-range coupling models [11, 14, 23, 24]. The long range coupling, globally coupling in particular, drives individual neurons to the averaged activity. Thus, the synchronization state can be easily achieved. But, as pointed out by Wang [25] and Terman & Wang [22], these long-range connections lead to indiscriminate segmentation since the network is dimensionless and loses critical geometrical information about the objects. So, desynchronization is very difficult to achieve and, as a consequence, the segmentation capacity is very small.

Mixed means the long-range coupling and local coupling coexist in the model, or the model is composed by various layers, and intralayer and interlayer neurons are coupled in a complex way. This approach have high biological plausibility. Usually, these kinds of models can be used not only for scene segmentation, but also to explain or simulate some phenomena of neuronal activities, such as neuronal synchronization, stimuli-evoked visual perception etc. [10, 15, 16]. However, it is hard to govern the dynamics in the networks. Thus, they are still not suitable to be applied to solve engineering scene segmentation problems.

From the viewpoint of engineering application of scene segmentation, locally coupled oscillatory correlation neural networks are more successful than others. The representative model of this kind is LEGION (Locally Excitatory Globally Inhibitory Oscillator Network) [2, 22, 25], since it offers rapid synchronization mechanism in a locally coupled oscillator group representing each object and, especially, offers an explicit desynchronization mechanism to separate a number of oscillator groups representing multiple simultaneously presented objects. However, the synchrony-desynchrony dilemma has not been avoided yet. In LEGION, neurons' local cooperation leads to synchronization, global competition leads to desynchronization. Each segment is represented by a synchronized periodic trajectory, and different groups of neurons oscillate with a phase shift. Because of the periodic nature, the chances of coincidence between two or more periodic trajectories (representing different objects) significantly increase as the number of objects to be segmented increases. Moreover, the synchronization and desynchronization analyses in these kinds of models are based on a limit cycle solution of the system [2, 21, 22]. Although each oscillator used in these models cannot be chaotic, the coupled system may be chaotic. Then, their analyses are not always valid since the chaotic range and the stable oscillating range in the parameter space have not been identified.

Up to now, to our knowledge, the maximum number of objects that can be segmented by an oscillatory correlation model is less than 12 [2, 22].

Chaos synchronization has been a topic of great interest since 1990 [17]. It has been recognized that it has potential applications for communication systems (for an extensive review, see [18]). In this paper, an oscillator network with diffusively coupled chaotic elements is presented. We show numerically that a large number of elements in such a lattice can be synchronized. Each object in a given scene is represented by a synchronized chaotic trajectory, and all such chaotic trajectories can be easily separated by utilizing the sensitivity and aperiodicity properties of chaos. Therefore, the synchrony-desynchrony dilemma can be avoided. As a consequence, our model has unbounded capacity of object segmentation. The differential equations are integrated by using the fourth-order Runge-Kutta method. Lyapunov exponents are calculated by using the algorithm presented by [29].

This paper is organized as follows. Sec. 2 describes chaotic dynamics in a single periodically driven Wilson-Cowan oscillator. Sec. 3 shows chaotic synchronization in a model of two-coupled chaotic Wilson-Cowan oscillators. Sec. 4 gives the model definition and the segmentation strategy. Computer simulations are shown in Sec. 5. Sec. 6 concludes the paper.

2. Chaotic Dynamics in a Periodically Driven Wilson-Cowan Oscillator

The Wilson-Cowan neural oscillator has been widely used in neural network modeling. Its stationary and periodic dynamics have been extensively studied [1, 2, 8, 12, 16, 23, 25]. It is considered not to be a single neuron but a meanfield approximation of neuronal groups. It is modeled as a feedback loop between an excitatory unit and an inhibitory unit:

$$\begin{aligned} \dot{x} &= -ax + G(cx + ey + I - \theta_x) \\ \dot{y} &= -by + G(dx + fy - \theta_y) \\ G(v) &= \frac{1}{1+e^{-(v/T)}} \end{aligned} \tag{1}$$

where a and b are decay parameters (positive numbers) of x and y, respectively; c and f are self-excitatory parameters; e is the strength of coupling from the inhibitory unit y to excitatory unit x, it is a negative value to assure that the variable y acts as inhibitory. The corresponding coupling strength from x to y is given by d. θ_x and θ_y are thresholds of unit x and y, respectively. $G(\bullet) \in [0, 1]$ is a sigmoid function and T defines its steepness. I is an external stimuli. If I is a constant, no chaos can appear since it is a two-dimensional continuous flow. In order to get a chaotic oscillator, the external stimuli is defined as a periodic function: $I(t) = A\cos(t)$, where A is the amplitude of the driven function.

In this paper, the amplitude of external stimulation A is considered a bifurcation parameter. Other parameters are held constant at: $a = 1.0$, $b = 0.01$, $c = 1.0$, $d = 0.6$, $e = -2.5$, $f = 0.0$, $\theta_x = 0.2$, $\theta_y = 0.15$, $T = 0.025$, as used in [25], in all the examples that appear in this text.

For characterizing the bifurcating and chaotic behavior, we consider the bifurcation diagram in Fig. 1-a, which shows the stroboscopic section of x at the fixed phase $A\cos(t) = 0$ against A.

From Fig. 1-a, we can see that periodic oscillation with period one occurs, when A is small. As A increases, a sequence of period-doubling bifurcation is observed. This bifurcation sequence accumulates at $A = 1.011$. For $A \geq 1.011$, chaotic behavior is observed. Fig. 1-b shows the largest Lyapunov exponents corresponding to Fig. 1-a. Especially, when $A = 1.2$, the largest Lyapunov exponent $\lambda_{max} = 0.037 > 0$, which indicates that the oscillator is chaotic at this parameter value.

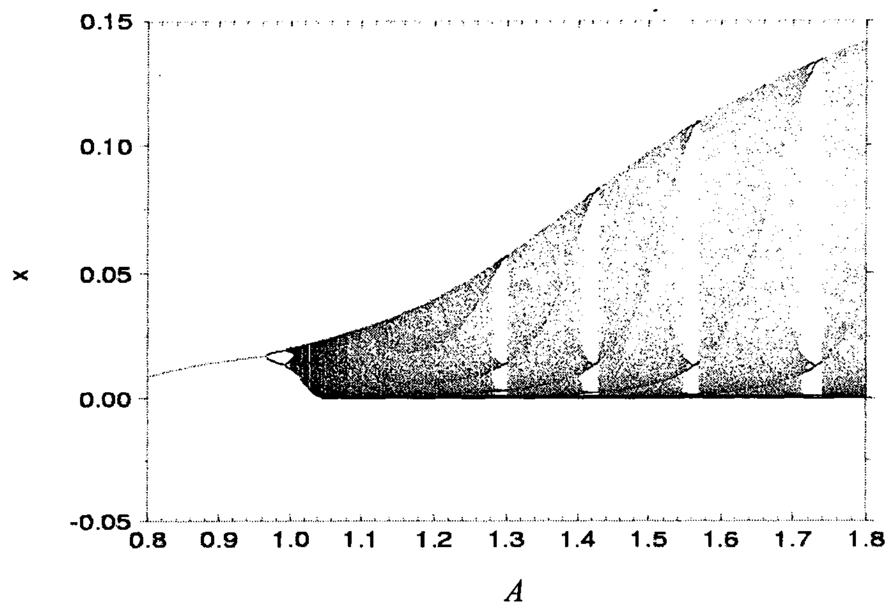

Fig. 1. Bifurcation diagram of periodically driven Wilson-Cowan oscillator by varying parameter A. The stepsize $\Delta A = 0.001$.

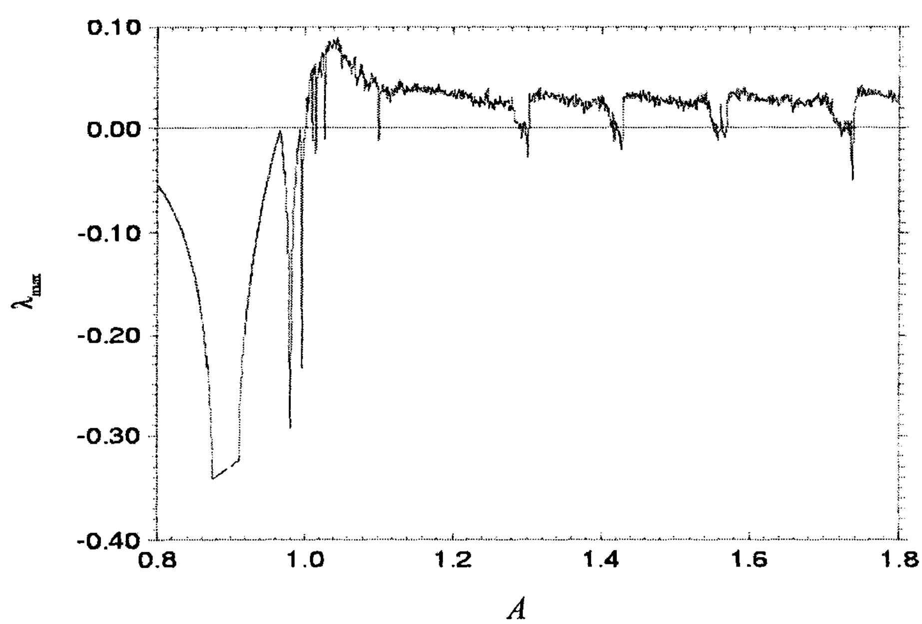

Fig. 2. Largest Lyapunov exponent against A. The stepsize $\Delta A = 0.001$.

3. Chaotic Synchronization in Two-Coupled Periodically Driven Wilson-Cowan Oscillators

The model of two linearly coupled Wilson-Cowan oscillators is defined by the following equations

$$
\begin{aligned}
\dot{x}_1 &= -ax_1 + G(cx_1 + ey_1 + A\cos t - \theta_x) + k(x_2 - x_1) \\
\dot{y}_1 &= -by_1 + G(dx_1 + fy_1 - \theta_y) + k(y_2 - y_1) \\
\dot{x}_2 &= -ax_2 + G(cx_2 + ey_2 + A\cos t - \theta_x) + k(x_1 - x_2) \\
\dot{y}_2 &= -by_2 + G(dx_2 + fy_2 - \theta_y) + k(y_1 - y_2) \\
G(v) &= \frac{1}{1+\exp[-(v/T)]}
\end{aligned}
\tag{2}
$$

where k is the coupling strength, and other parameters were the same as previously stated.

Fig. 3-a shows the average difference between the variables x of the two oscillators in relation to the coupling strength. Two oscillators run from different initial conditions. One can see from that figure that the two elements do not synchronize when the coupling strength is very small and they synchronize when the coupling strength is beyond a certain value. Fig. 3-b shows the same thing in the case when each oscillator is given a random small perturbation. The perturbation is switched on at $T = 50$ and switched off at time $T = 100$. Again, two oscillators can be synchronized by providing a larger coupling strength. The perturbation mechanism will be used in our model to distinguish one chaotic trajectory from another.

a)

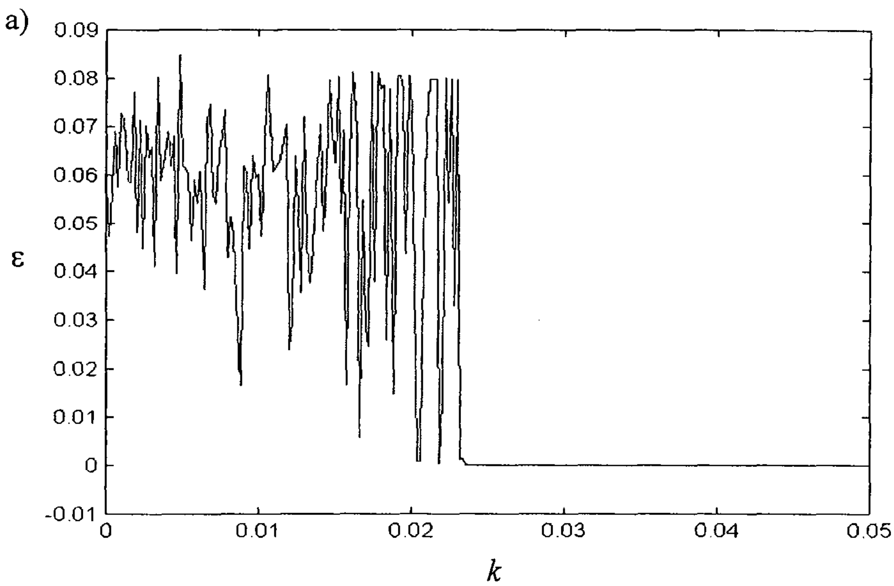

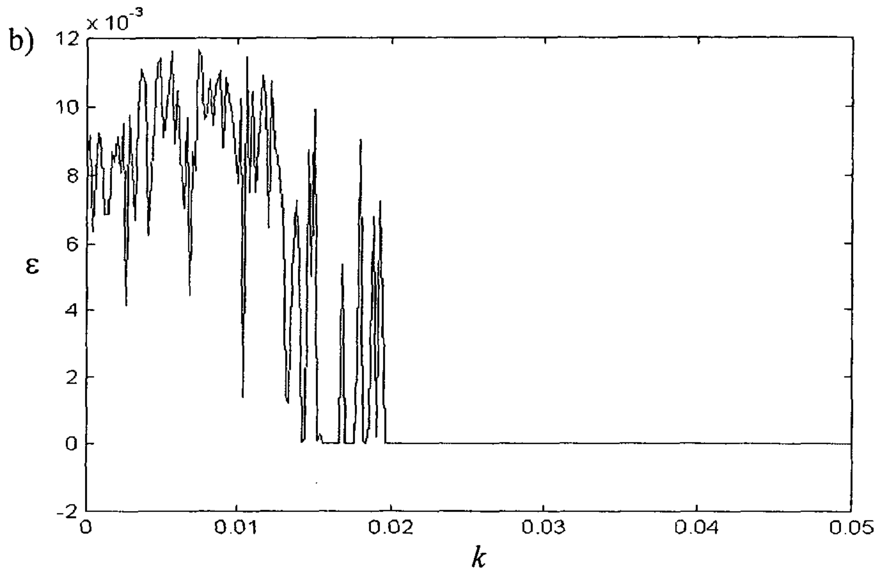

Fig. 3. Average difference between variable x of the two oscillators against the coupling strength k. The stepsize $\Delta k = 0.0002$. a) unperturbed solution; b) each x variable of the two oscillators receives a random perturbation. The amplitude of perturbations is of the order of 10^{-3}.

4. Model Description

Our model is a two dimensional network. Each node is a chaotic Wilson-Cowan oscillator. It is governed by the following equations:

$$\begin{aligned} \dot{x}_{i,j} &= -ax_{i,j} + G\left(cx_{i,j} + ey_{i,j} + I_{i,j} - \theta_x\right) + k\Delta x_{i,j} + \sigma_{i,j} \\ \dot{y}_{i,j} &= -by_{i,j} + G\left(dx_{i,j} + fy_{i,j} - \theta_y\right) + k\Delta y_{i,j} \\ G(v) &= \frac{1}{1+e^{-(v/T)}} \end{aligned} \tag{3}$$

where (i, j) is a lattice point with $1 \le i \le M$, $1 \le j \le N$, M and N are the lattice dimensions. $\sigma_{i,j}$ is a small perturbation term, which will be discussed below. k is the coupling strength. $\Delta x_{i,j}$ is the coupling term from other excitatory units. $\Delta y_{i,j}$ is the coupling term from other inhibitory units. These terms are given by

$$\Delta u_{i,j} = \Delta^{+} u_{i,j} + \Delta^{\times} u_{i,j} \tag{4}$$

where Δ^{+} and $\Delta^{\times}$ are two discrete two-dimensional Laplace operators given respectively by + and × shaped stencils on the lattice [4], that is, by

$$\Delta^{+}u_{i,j} = u_{i+1,j} + u_{i-1,j} + u_{i,j+1} + u_{i,j-1} - 4u_{i,j}$$
$$\Delta^{\times}u_{i,j} = u_{i+1,j+1} + u_{i-1,j+1} + u_{i+1,j-1} + u_{i-1,j-1} - 4u_{i,j} \quad (5)$$

So, each lattice element is connected to its 8 nearest neighbors. The boundary condition is free-end, that is,

$$x_{i,j} = 0,\ y_{i,j} = 0, \text{ if either } i \le 0, \text{ or } j \le 0, \text{ or } i \ge M+1, \text{ or } j \ge N+1. \quad (6)$$

One can easily see that the interaction terms will vanish i.e., $\Delta x_{i,j} = 0$ and $\Delta y_{i,j} = 0$, when the oscillators are synchronized. Thus, the synchronous trajectory will remain once the synchronization state is achieved.

The segmentation strategy is described below. Considering a binary scene image containing p non-overlapped objects. The network is organized that each element corresponds to a pixel of the image. The parameters can be chosen so that the stimulated oscillators (receiving a proper input, corresponding to a figure pixel) is chaotic. The unstimulated oscillators (receiving zero or a very small input, corresponding to a background pixel) remain silent ($x_{i,j} = 0$). If each group of connected, stimulated oscillators synchronize in a chaotic trajectory, then each object is represented by a synchronized chaotic orbit, namely X_1, X_2, ..., X_P. From the calculation of Lyapunov exponents in Sec. 3, we know that the dynamics of each synchronized chaotic orbit is qualitatively similar to a single uncoupled oscillator under this coupling scheme. Thus, X_1, X_2, ..., X_P can be considered as a series of orbits generated by a same chaotic system and running from same or different initial conditions. Due to the sensitive dependency on initial condition, which is the main characteristic of chaos, if we give a different (or random) small perturbation to each trajectory of X_1, X_2, ..., X_P, i.e., $X_1+\delta_1$, $X_2+\delta_2$, ..., $X_P+\delta_2$, all these chaotic orbits will be exponentially distant from each other after a while. This is equivalent to giving a perturbation to each stimulated oscillator as shown in Eq. (3). On the other hand, the synchronization state would not be destroyed by a small perturbation if it was an asymptotically stable state. In this way, all the objects in the scene image can be separated. From the above description, one can see that the segmentation mechanism is irrespective to the number of objects in a given scene. Thus, our model has unbounded capacity of segmentation.

Computer simulations show that objects in a given scene can be separated (resulting synchronized chaotic trajectories are distinct) even without the perturbation mechanism.

Fujisaka & Yamada [7] and Heagy *et al.* [13] have proved analytically that a one-dimensional array of diffusively coupled chaotic elements can be synchronized and the synchronization state is asymptotically stable by providing large enough coupling strength. Moreover, under this coupling scheme, the synchronized orbit will be periodic if all the elements are periodic; it will be chaotic if at least one element is chaotic. This analysis can be extended to a two dimensional lattice and the conclusions are still maintained.

5. Computer Simulations

In the following computer simulation, each stimulated oscillator (corresponds to a figure pixel) receives an external input with amplitude A =1.2. Unstimulated oscillators (corresponds to a background pixel) have A = 0.0. From the analysis of a single oscillator in Sec. 2, we know that each stimulated oscillator will be chaotic, while those without stimulation will remain silent.

In order to verify the superior segmentation capacity of this model, a computer simulation is performed with an input pattern containing 16 objects as shown in Fig. 4. Some objects have identical size and shape. The input image is again presented on a 25×25 oscillator grid. The coupling strength is k = 6.5. Fig. 5 shows the temporal activities of the oscillator blocks. We can see the appearance of 16 synchronized chaotic orbits each of which represents an isolated object. The 16 orbits have mutually different temporal behavior.

Different groups of oscillators can reach the active phase at the same time. Therefore, usually we cannot correctly extract objects by only evaluating their activities at an instant. A formal method for extracting objects is to calculate cross-correlation among neurons in a certain time window. However, this is computationally demanding because a large number of neurons are involved. Here, we propose a simple method incorporating the characteristics of chaos.

The method works as follows: we know that different chaotic trajectories may cross a predefined Poincaré section simultaneously at some instant. However, because of the sensitive dependency property of chaos, they cannot keep together for a long time. Moreover, they separate rapidly once they have approached. Then, these chaotic trajectories can be distinguished by keeping observing their second, third or more crossing of the Poincaré section. If a set of oscillators cross the Poincaré section simultaneously on several successive times, they are considered to be a segmented object. For this purpose, a proper time interval is chosen within which each chaotic trajectory can cross the Poincaré section several times (3 or 4 times are sufficient). In this method, one object is extracted in each time interval.

Now, let the oscillators synchronize and desynchronize (round off the transient phase). During the first time window, a set of oscillators that first crosses the Poincaré section is denoted as E_1. E_1 may be composed of one or several objects. Anyway, an object included in E_1 will be extracted. At another instant, a set of oscillators E_2 crosses the Poincaré section. Note that individually E_1 or E_2 may be associated to different objects. Now, we check the intersection of E_1 and E_2, if $E_1 \cap E_2 = \phi$, i.e., E_1 and E_2 are two sets of oscillators containing completely different objects, that is, the object which will be extracted in this time interval is not contained in E_2, then E_2 is ignored and we continue observing the next crossing. Otherwise, if $E_1 \cap E_2 \neq \phi$, then, the content of E_1 is replaced by the intersection of E_1 and E_2, i.e., $E_1 \leftarrow E_1 \cap E_2$. As the system is running, a third set of oscillators will cross the Poincaré section, say E_3. Again, we check the intersection between the possibly modified E_1 and the new set E_3: if $E_1 \cap E_3 = \phi$, we only wait for the next crossing; if $E_1 \cap E_2 \neq \phi$, then, $E_1 \leftarrow E_1 \cap E_3$. This process continues until the end of the current time interval is reached. Now,

$E_1 = E_1 \cap E_2 \cap \ldots \cap E_L$, where $E_1, E_2, \ldots, E_L$ are the crossing sets which have common elements. The markers associated with these selected oscillators are set to a special symbol and, these oscillators will not be processed further. Just after the first time interval, the second starts. The same process is repeated and the second object is extracted. This process continues until all activated oscillators are marked with the special symbol. Finally, the whole process terminates and all objects in the scene are extracted.

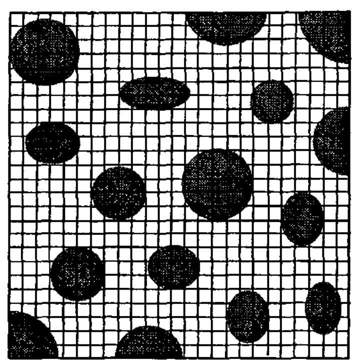

Fig. 4. An input pattern with 16 objects (black figures) mapped to a 25×25 oscillator network.

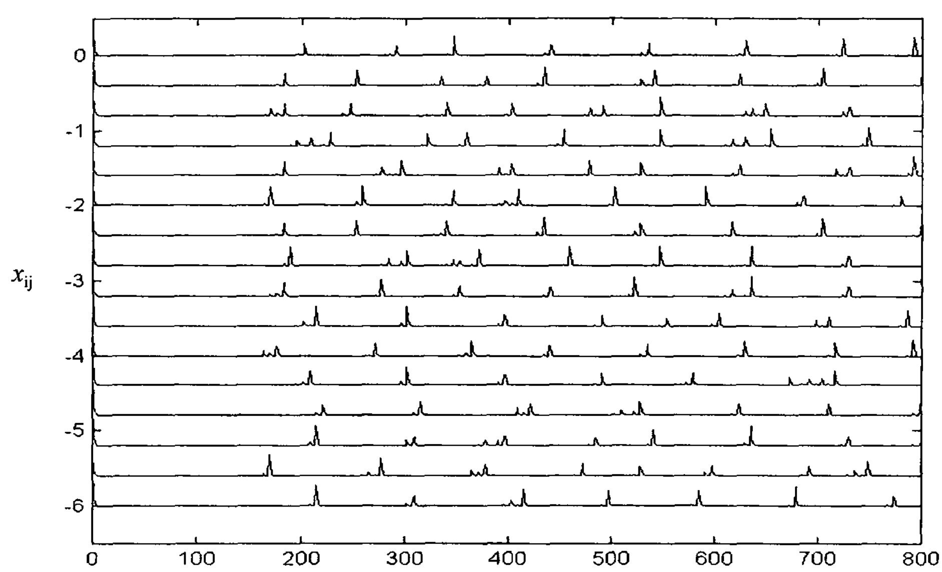

Fig. 5. Temporal activities of oscillator blocks (unperturbed solution). Each trace in the figure is a synchronized chaotic orbit, which contains elements corresponding to an object in the input pattern. Vertical scale of second to twentieth oscillator blocks are shifted downwards by 0.4.

Figure 6 shows the result of object extraction by utilizing the above introduced method. The input pattern is again shown by Fig. 6. The Poincaré section is defined as $x_{ij} = 0.05$. The time interval of length 300 is chosen. Elements represented by a same symbol means that they are extracted at the same time interval. Then, they are considered as a single object; elements represented by different symbols means they are extracted at different time intervals and, consequently, they are considered as elements in different objects. One can easily see that the 16 objects are correctly extracted by comparing with the input pattern.

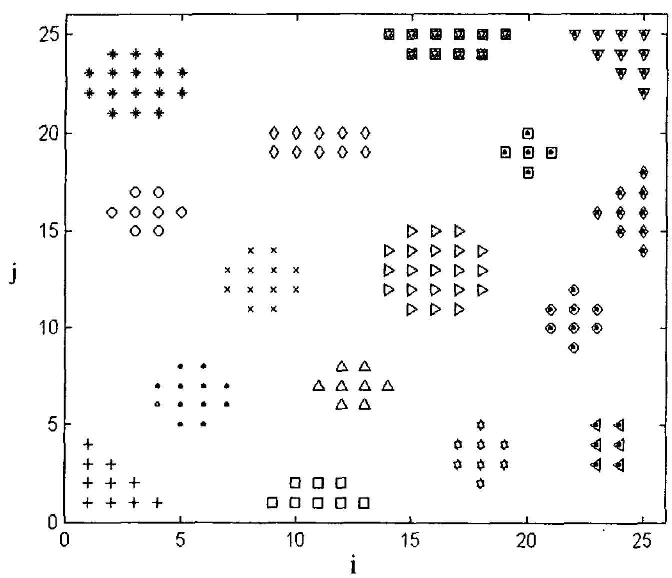

Fig. 6. Objects extracted by the simple method presented in the text.

6. Conclusions

Besides the complexity of chaotic systems, they can synchronize if proper conditions are held. On the other hand, sensitive dependence on initial condition implies that two nearby trajectories will diverge exponentially in time. Thus, chaos is a suitable solution to escape from the synchrony-desynchrony dilemma.

For the segmentation of a gray level image with overlapped objects, the amplitude of external stimulation of each oscillator can be arranged to take different values, i.e., oscillators represent different gray level pixels will be in different chaotic states. The coupling strengths among neurons are taken as an all-or-nothing filtering scheme, i.e. the coupling between pixels with small gray level difference will be maintained, while the coupling between pixels with great gray level difference will be cut. Other techniques are the same as used in the model for binary image segmentation. The results will be reported elsewhere.

It should be noted that our model is limited to arrays of symmetrically coupled identical chaotic oscillators, and therefore, the only synchronization phenomenon that can be found is the complete synchronization. It is known that non-identical symmetrically coupled chaotic oscillators can give rise to weak synchronization feature, such as phase and lag synchronization [19, 20]. It is interesting to incorporate these phenomena to build a more realistic and robust model.

Finally, we think that the simulation results of the model are consistent with our everyday experience. Let's consider a visual scene. We can see many stars in the sky on a summer night, but not only few of them. Why? It is only possible that all the stars we see have been firstly separated from one another, then recognized by our visual and central neural systems. Although we cannot pay attention to many things at a given instant, the underlying capacity of visual segmentation of human (animal) is unidentifiably large.

References

1. Baird, B.: Nonlinear dynamics of pattern formation and pattern recognition in the rabbit olfactory bulb, Physica 22D, (1986) 150-175.
2. Campbell, S. & Wang, D. L.: Synchronization and Desynchronization in a Network of Locally Coupled Wilson-Cowan Oscillators, IEEE Trans. Neural Networks, 7(3), (1996) 541-554.
3. Chen, K. & Wang, D.-L.: Perceiving without Learning: from Spirals to Inside/Outside Relations, Technical Report, OSU-CISRC-8/97-TR38 (1997).
4. Chow, S.-N & Mallet-Paret, J.: Pattern Formation and Spatial Chaos in Lattice Dynamical Systems – Part I, IEEE Trans. Circuits Syst. I, 42(10), (1995) 746-751.
5. Eckhorn, R., Bauer, R., Jordan, W., Brosch, M., Kruse, W., Munk, M. & Reitboeck, H. J.: Coherent oscillation: A mechanism of feature linking in the visual cortex?, Biol. Cybern. 60, (1988) 121-130.
6. Engel, A. K., König, P., Kreiter, A. K & Singer, W.: Interhemispheric Synchronization of Oscillatory Neuronal Responses in Cat Visual Cortex, Science, 252, (1991) 1177-1178.
7. Fujisaka, H. & Yamada, T.: Stability theory of synchronized motion in coupled-oscillator systems, Progress of Theoretical Physics, 60(1), (1983) 32-47.
8. Fukai, T.: Synchronization of neural activity is a promising mechanism of memory information processing in networks of columns, Biol. Cybern., 71, (1994) 215-226.
9. Grey, C. M., König, P., Engel, A. K. & Singer, W.: Oscillatory responses in cat visual cortex exhibit inter-columnar synchronization which reflects global stimulus properties, Nature, 338, (1989) 334-337.
10. Grossberg, S. & Somer, D.: Synchronized oscillations during cooperative feature linking in a cortical model of visual perception, Neural Networks, 4, (1991) 453-466.
11. Hansel, D. & Sompolinsky, H.: Synchronization and Computation in a Chaotic Neural Network, Phys. Rev. Lett., 68(5), (1992) 718-721.
12. Hayashi, Y.: Oscillatory Neural Network and Learning of Continuously Transformed Patterns, Neural Networks, 7, (1994) 219-231.

13. Heagy, J. F., Carroll, T. L. & Pecora, L. M.: Synchronous chaos in coupled oscillator systems", Phys. Rev. E, 50(3), (1994) 1874-1885.
14. Kaneko, K.: Relevance of dynamic clustering to biological networks, Physica D, 75, (1994) 55-73.
15. König, P. Schillen, T. B.: Stimulus-dependent assembly formation of oscillatory responses. I Synchronization, Neural Computation, 3, (1991) 155-166.
16. König, P. Schillen, T. B.: Binding by temporal structure in multiple feature domains of an oscillatory neuronal network, Biol. Cybern. 70, (1994) 397-405.
17. Pecora, L. M. & Carroll, T. L.: Synchronization in chaotic systems, Phys. Rev. Lett. 64, (1990) 821-823.
18. Pecora, L. M., Carroll, T. L., Johnson, G. A., Mar, D. J. & Heagy J. F.: Fundamentals of synchronization in chaotic systems, concepts, and applications, Chaos, 7(4), (1997) 520-534.
19. Rosenblum M. G., Pikovsky A. S. & Kurths J.: Phase Synchronization of Chaotic Oscillators, Phys. Rev. Lett., 76(11), (1996) 1804 - 1807.
20. Rosenblum M. G., Pikovsky A. S. & Kurths J.: From Phase to Lag Synchronization in Coupled Chaotic Oscillators, Phys. Rev. Lett., 78(22), (1997) 4193 - 4196.
21. Somer, D. & Kopell, N.: Rapid synchronization through fast threshold modulation, Biol. Cybern. 68, (1993) 393-407.
22. Terman, D. & Wang, D.-L.: Global competition and local cooperation in a network of neural oscillators, Physica D, 81, (1995) 148-176.
23. von der Malsburg, Ch. & Buhmann, J.: Sensory segmentation with coupled neural oscillators, Biol. Cybern., 67, (1992) 233-242.
24. von der Malsburg, Ch. & Schneider, W.: A Neural Cocktail-Party Processor, Biol. Cybern., 54, (1986) 29-40.
25. Wang, D.-L.: Emergent Synchrony in Locally Coupled Neural Oscillators, IEEE Trans. Neural Networks, 6(4), (1995) 941-948.
26. Wang, D.-L.: Object Selection Based on Oscillatory Correlation, *Technical Report*, OSU-CISRC-12/96 - TR67 (1996).
27. Wang, D.-L.: Primitive auditory segregation based on oscillatory correlation, Cognitive Science, 20, (1996) 409-456.
28. Wang, D.-L. & Terman, D.: Image Segmentation by Neural Oscillator Networks, IEEE Trans. Neural Networks, (1996) 1534-1539.
29. Wolf, A., Swift, J. B., Swinney, H. L. & Vastano, J. A.: Determining Lyapunov Exponents From a Time Series, Physica 16D, (1985) 285-317.

NOTAS DO ICMC

SÉRIE COMPUTAÇÃO

056/2000 BATISTA, G E A P A; CARVALHO, A C P L F; MONARD, M C – Applying one-sided selection to unbalanced datasets.

055/2000 NONATO, L G; MINGHIM, R.; OLIVEIRA, M C F; TAVARES, G. – A novel approach for delaunay 3D reconstruction with a comparative analysis in the light of applications.

054/2000 MORSELLI JR., J C M; SANTANA, R H C; SANTANA, M J; ULSON, R S – An approach for dynamic swapping of distributed simulation synchronisation protocols.

053/2000 SPOLON, R.; SANTANA, M J; SANTANA, R H C – A methodology for performance evaluation of optimistic distributed simulation synchronisation mechanisms.

052/2000 BRANCO, K R L J C; SANTANA, M J; SANTANA, R H C; CALÔNEGO JUNIOR, N – A parallel programming supporting tool.

051/2000 FRANCÊS, C R L; VIJAYKUMAR, N L; SANTANA, M J; CARVALHO, S V de; SANTANA, R H C – Stochastic statecharts for obtaining performance measurements of a file server model.

050/2000 FARIA,G; ROMERO, R A F – Incorporating fuzzy logic to reinforcement learning.

049/2000 OLIVEIRA, P R; ROMERO, R F; NONATO, L G; MAZUCHELI, J – Techniques for image compression: a comparative analysis.

048/2000 LINS, L; LINS, S; MORABITO, R – Na n-tet graph approach for non-guillotine packings of n-dimensional boxes into na n-container.

047/2000 OLIVEIRA JR., O N; MARCHI, A R; MARTINS, M S; MARTINS, R T; NUNES, M G V – A critical analysis of the performance of english-portuguese-english MT systems.